

74p
NASA CR-132946

(Final Report)

ANALYTICAL TOOLS
AND ISOLATION OF TOF EVENTS

H. Wolf

(NASA-CR-132946) ANALYTICAL TOOLS AND
ISOLATION OF TOF EVENTS Final Report
(Analytical Mechanics Associates, Inc.)
23 p HC \$4.25 CSCI 12A

N74-20175

G3/19 Unclass
34274

AMA Report Nos. 74-5 and 73-45
Contract NAS5-11992
January 1974

ANALYTICAL MECHANICS ASSOCIATES, INC.
9430 LANHAM SEVERN ROAD
SEABROOK, MARYLAND 20801

SUMMARY

This final report consists of two reports concerning analytical tools. The first report is entitled, "Probability Analysis of the Orbital Distribution of Events". It was included as an Appendix in AMA Report No. 73-44 (October 1973). The second report is entitled, "Particle Trajectories for a Repulsive Force Field". These two reports summarize the work done on Task III of the subject contract.

The work on Task IV was included as a modification to the program reported in AMA Report No. 73-44 (Statistical Information Program, Progress Report, (Task II)), October 1973.

The modification works fully automatically and points out TOF events. The modified program has been checked thoroughly and delivered to the Technical Officer. So far, two TOF events were discovered.

The work on Task III and IV of the subject contract has thus been completed and will be invoiced.

PROBABILITY ANALYSIS OF THE ORBITAL
DISTRIBUTION OF EVENTS

H. Wolf

AMA Report No. 74-5
Contract NAS5-11992
January 1974

PRECEDING PAGE BLANK NOT FILMED

ANALYTICAL MECHANICS ASSOCIATES, INC.
10210 GREENBELT ROAD
SEABROOK, MARYLAND 20801

Table of Contents

	<u>Page</u>
Introduction	1
Analysis	1
Application to Actual Orbital Distribution	2
Conclusions	4
References	4

PROBABILITY ANALYSIS OF THE ORBITAL
DISTRIBUTION OF EVENTS

1. Introduction.

The fine structure of the dust flux density may be examined by noting asymmetries in the event rate. The analysis contained herein permits a distinction between asymmetries caused by random fluctuations and systematic variations by calculating the probability of any particular asymmetry. The analysis is applied to an asymmetry observed in Pioneer 8 and 9 distributions.

2. Analysis.

Let the relative probability of an event occurring in the half orbit H_T as the spacecraft is moving toward the solar apex be p , and in the other half orbit H_A be q , where $p + q = 1$.

If n events are observed altogether, the probabilities of all possible combinations are given by the terms of the binomial expansion

$$(p+q)^n = p^n + \binom{n}{1} p^{n-1} q + \binom{n}{2} p^{n-2} q^2 + \dots \quad (1)$$

Thus the first term in the expansion gives the probability of all events occurring in H_T , the second term the probability of all except one of the events occurring in H_T , etc. Other probabilities may be obtained by summing appropriate terms in the expansion (1). For instance, the probability of at least γ of the events occurring in H_T (i.e., at most $n-\gamma$ events in H_A) is given by the sum

$$\sum_{k=0}^{n-\gamma} \binom{n}{k} p^{n-k} q^k. \quad (2)$$

It is apparent that for large values of n , the computation of the numerous terms involved in (2) may be extremely laborious. However, for $npq \gg 1$ an adequate approximation to the binomial distribution is given by:

$$\binom{n}{k} p^k q^{n-k} \approx \frac{1}{\sqrt{2\pi npq}} e^{-(k-np)^2/2npq}$$

(See Reference 1);

i. e., the binomial distribution may be approximated by a Gaussian distribution of mean np and standard deviation \sqrt{npq} .

Instead of summing the terms involved, in an expression such as (2), we may use the corresponding extensively tabulated integrals of the normal curve.

3. Application to Actual Orbital Distribution.

The actual distribution for Pioneer 8 events was found to be:

Total number of events analyzed:	230
Events in H_T (moving toward s.a.)	139
Events in H_A	91

Corresponding numbers for Pioneer 9

Total number of events analyzed:	111
Events in H_T	73
Events in H_A	38

Combined totals:

Total number	341
in H_T	212
in H_A	129

As a working hypothesis it is assumed $p = q = .5$ (i. e., the probability of an event occurring is the same for each half orbit).

For Pioneer 8. The expected number in each half orbit is then $np = 115$ and the deviation from this expected number is $139 - 115 = 24$, thus for this case $\sigma = \sqrt{230 \cdot \frac{1}{2} \cdot \frac{1}{2}} = 7.58$. Consequently, we have a deviation of 3.17σ , corresponding to a probability of 0.16%.

For Pioneer 9 the deviation from the mean is 17.5 and the standard deviation is 5.27 resulting in a deviation of 3.32σ . This corresponds to a probability of 0.08%.

It is realized, of course, that the time spent in each of the half orbits is not the same. Pioneer 8 spends 578 days in H_T and 507 days in H_A corresponding to a daily event rate of .240/day and .179/day, respectively. If we increase the time in H_A by 71 days and hypothesize that the daily event rate holds this would indicate 13 additional events occurring in the half orbit H_A .

So, the new hypothetical distribution would be:

(Pioneer 8)

Total number of events	243
Events in H_T	139
Events in H_A	104

$$np = 121.5$$

$$d = 17.5$$

$$\sigma = 7.79$$

Thus $d = 2.24\sigma$, corresponding to a probability of 2.5%.

For Pioneer 9, the event rate in H_A was .113 and the number of days spent in H_T and H_A was 355 and 335, respectively.

Making a same adjustment as above the additional 20 days would lead to an additional 2 events in H_A . Thus, the new hypothetical distribution would be:

(Pioneer 9)

Total number of events	113
Events in H_T	73
Events in H_A	40

$$\text{Expected number, } np = 56.5.$$

With the deviation $d = 16.5$, and the standard deviation $\sigma = 5.32$, then $d = 3.10 \sigma$. This corresponds to a probability of 0.2%.

The combined results are tabulated as:

Hypothetical:

Pioneer 8 and 9

Total number of events:	356
Events in H_T	212
Events in H_A	144

Expected number of events in each half orbit: 178

$$d = 212 - 178 = 34$$

$$\sigma = 9.43$$

$$d = 3.61 \sigma,$$

corresponding to a probability of 0.04%.

4. Conclusions.

It is seen that the probability for random variations to produce the observed asymmetry in the distribution of events is very small. Then, the observed asymmetry should be attributed to some systematic effect, such as the presence of interstellar grains.

5. References.

- [1] "Probability, Random Variables, and Stochastic Processes", Athanasios Papoulis (Polytechnic Institute of Brooklyn). McGraw-Hill Series in Systems Science. Copyright 1965.

PARTICLE TRAJECTORIES FOR A
REPULSIVE FORCE FIELD

H. Wolf
J.B. Eades, Jr.

AMA Report No. 73-45
Contract NAS5-11992
October 1973

PRECEDING PAGE BLANK NOT FILMED

ANALYTICAL MECHANICS ASSOCIATES, INC.
10210 GREENBELT ROAD
SEABROOK, MARYLAND 20801

//

Table of Contents

	<u>Page</u>
Introduction	1
Computational Sequence	3
Typical Results	6
Reference	13

Introduction

Under simple assumptions the force on a particle due to solar radiation pressure is directed along the particle's radius vector, from the sun, and is inversely proportional to its distance from the sun. In addition the force is assumed proportional to the cross sectional area of the particle. Thus the particle's acceleration due to radiation pressure is given by:

$$\frac{C_{\odot} A}{m} \frac{R}{r^3}$$

and the equation of motion of the particle subject to both solar radiation pressure and gravitational attraction is given by:

$$\ddot{R} = -\mu_{\odot} \frac{R}{r^3} + \frac{C_{\odot} A}{m} \frac{R}{r^3} = -\mu_{\odot} (1 - \beta) \frac{R}{r^3} \quad (1)$$

where:

R is the radius vector of the particle
 r its magnitude ($= |R|$)

μ_{\odot} the sun's gravitational constant ($= K^2 M_{\odot}$)

C_{\odot} the force due to solar radiation pressure on a particle of unit cross sectional area at unit distance

A the cross sectional area of the particle

m particle mass

$$\beta = \frac{C_{\odot} A}{\mu_{\odot} m} \quad (2)$$

If the particle is assumed approximately spherical then

$$\frac{A}{m} = \frac{\pi a^2}{\frac{4}{3} \pi a^3 \rho} = \frac{3}{4a\rho} \quad (3)$$

where

a is the particle radius and

ρ its density

thus

$$\beta = \frac{3C_{\odot}}{4\mu_{\odot}} \frac{1}{\rho a} = \frac{k}{(m\rho)^{2/3}} \quad (4)$$

defining the constant k as:

$$k \equiv \left(\frac{9\pi}{16}\right)^{1/3} \frac{C_{\odot}}{\mu_{\odot}} ;$$

For large, dense particles $\beta \ll 1$; consequently the normal Keplerian orbit for such a particle would only be slightly modified. As the particle radius or density decrease β will increase and may, for sufficiently small, light particles, exceed 1. In this case the net force will be repulsive.

Kepler's theory may be modified for these cases. The motion then takes place along the branch of the hyperbola which is convex toward the focus occupied by the sun.

For situations such as these there will be a "forbidden zone" about the sun into which these particles may not penetrate. The zone is of course dependent on the "velocity at infinity", the radiation pressure and the angular momentum of the particle. It is the purpose of this note to develop a sketch of this "forbidden zone".

The value of the radiation pressure constant used here, has been chosen to be consistent with that given by Silverberg. (Reference [1]).

The attractive and repulsive cases are separated by $\beta = 1$; since here the particle moves in a force free field. For a particle of given mass this gives rise to a "limiting" density; or, for a particle of given density, to a "limiting" mass or diameter. Particles with densities (or masses) smaller than their limiting values are repelled, others are attracted.

As an example: for a particle of mass 8.9×10^{-13} grams (similar to that for event 20 from Pioneer 8) the limiting density of 0.953 gr/cc.

For a particle with a (very likely) density (ρ) of 3 gr/cc, its limiting diameter would be 3.85×10^{-5} cm, and it would have a corresponding limiting mass of 8.99×10^{-14} gr.

For the curves plotted and presented herein, a density of 3 gr/cc and an excess speed (V_{∞}) of 20 km/sec (corresponding to the velocity of the solar system)

has been assumed. (Of course, corresponding curves for other values of these parameters can readily be obtained).

A word description of the trajectory "flown" by a test particle in the presence of the assumed solar mass-radiation influence is given below. In addition, there is a sketch included here to show several geometric properties of the trajectory.

The flight paths of interest are those which describe hyperbolae in the vicinity of the sun. These particles are assumed to "arrive" in the solar system with an excess speed (V_{∞}) of 20 km/sec (the assumed value). If these particles approach the sun not along a direct radius, but at some offset distance (i.e., with non-zero angular momentum), then they will describe hyperbolic arcs which can be predicted from the two-body model described above. On the sketch, below, "q" is the closest solar approach distance; c is the off-set distance (measured from the solar apex radial), and \bar{V}_{∞} is the approach excess velocity. Also, as shown on the figure, θ is an angle locating the hyperbola's axis measured from the solar apex radial. Due to symmetry, these hyperbolae may be oriented symmetrically about the radial. Thus there could be mirrored images of each path on this principal radius.

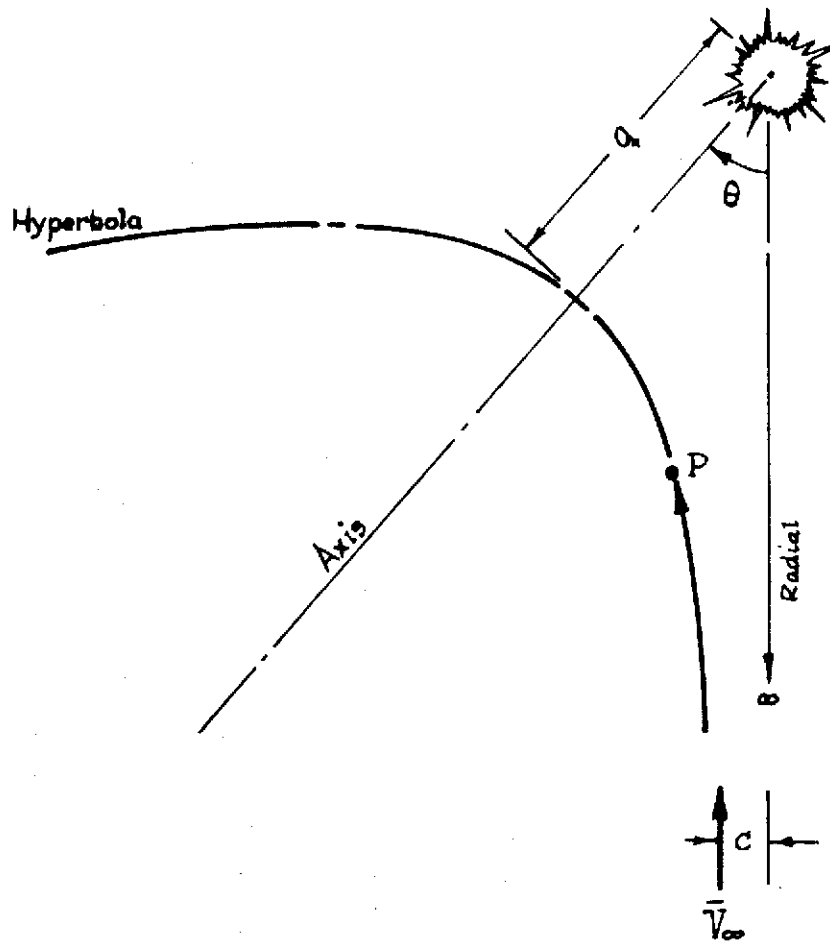
Computational Sequence

In determining geometric characteristics of these trajectories, and obtaining a description of the FORBIDDEN ZONE, the following calculations procedure has been utilized.

(1). A density of $\rho = 3$ gr/cc is assumed; knowing m_{lim} (the limit mass), choose values for the particle mass ($m < m_{lim}$).

(2). With k known, ($9.32 * 10^{-5}$) and having chosen ρ then calculate a β corresponding to each m; i.e., from (4)

$$\beta \equiv \frac{(9.32 * 10^{-5})}{(\rho^2 m)^{1/3}}, \quad (\rho \equiv 3.0).$$



Sketch depicting a particle (P) moving from ∞ , with a velocity \bar{V}_∞ , offset at a distance c , which has a closest approach (q) to the sun (μ), as shown.

This closest approach depends on the quantities μ , c , V_∞ .

The path for P is a hyperbola (for this repulsive system); the axis of the hyperbola is inclined at an angle θ from the radial (to ∞). Here, θ is dependent on the parameters μ , c , V_∞ .

Note: Here, $\beta \geq 1.0$, by definition.

(3). Having obtained β , calculate the equivalent μ (sun value) for the system:

$$\mu = \mu_{\odot} (1 - \beta),$$

with $\mu_{\odot} \equiv 2.959 * 10^{-4} \text{ (AU}^3/\text{DA}^2\text{)}$.

(4). Next, assuming $V_{\infty} = 20 \text{ km/sec}$, calculate the parameter, B, where:

$$B \equiv \frac{-\mu/c}{V_{\infty}^2}.$$

And, (5). Knowing B define characteristics for the hyperbolic path; e.g.:

$$\theta \equiv \tan^{-1} \left(\frac{V_{\infty}^2}{-\mu/c} \right) = \tan^{-1} \left(\frac{1}{B} \right)$$

and

$$\begin{aligned} \frac{q}{c} &\equiv \frac{-\mu/c}{V_{\infty}^2} + \left[1 + \left(\frac{-\mu/c}{V_{\infty}^2} \right)^2 \right]^{1/2} \\ &= B + \left[1 + B^2 \right]^{1/2}. \end{aligned}$$

These data may be used to plot a boundary defining closest approaches to the sun, for various system constraints and/or conditions. However, the FORBIDDEN ZONE, as defined, is not yet obtained. This region of "space" lies on the sun's side of the geometric envelope for the family of hyperbolae traced out by the assumed particles. In this regard, then, it is necessary to examine the problem (mathematically or graphically) and to define the envelope accordingly.

Since the model used for the present investigation leads to analytical results, the envelope curve can be described mathematically. For this description the parameter (A) is introduced, wherein $A \equiv \frac{1}{B}$ (see above), and the equations for the trajectory are rewritten. Making use of the formal operations to determine an envelope, it can be shown that the pair of parametric cartesian equations for this curve are:

$$x = \frac{(A_y)^2 \left[1 - \sqrt{1 + A^2} \right] - y^2 + 2 (Ac)^2 \left[1 + \sqrt{1 + A^2} \right]}{(Ay) \left[\sqrt{1 + A^2} - 2 \right]}$$

and

$$y = \pm c \left\{ \frac{(2 + 3A^2) \left[1 + \sqrt{1 + A^2} \right] + A^2}{\left[1 + A^2 \right]^{3/2}} \right\}^{\frac{1}{2}}$$

For these expressions the x-axis parallels the solar-apex radial; and its positive direction is in the apex direction. The y-axis is normal to x; it may be assigned signs of \pm arbitrarily. (Recall that c is the off-set distance -- for \bar{V}_∞ -- expressed as a distance, measured in AU. Consequently, the coordinates (x, y) are similarly dimensioned).

Typical Results

Table I shows: (1), a summary for the calculations outlined above. Here one will find tabulated, as a function of m, the corresponding values for β and μ (see Eqs. (2) and (3)).

Also, in the table, is a listing of closest approach distance (q_{\min}) for each of the m values selected. The quantity q_{\min} (in AU) denotes the closest distance that a particle of mass m can approach the sun under the conditions assumed. Necessarily, these distances correspond to an offset distance (c) of zero.

Next, for a unit offset distance (i.e., $c = 1.0$ AU), typical values of q (AU) and θ (deg) are tabulated. These data are illustrative of the results which may be expected from the calculations procedure outlined earlier.

Lastly, there is a listing of c(AU) values which are required to attain a $q = 2.0$ AU (for each value of m defined). Since $q = 2$ AU has been arbitrarily chosen as an upper bound of interest, here, then these data define a practical

upper limit for the present investigation. (Note: when the notation $c < 0$ is used herein it infers that these particles cannot have a q_{\min} as small as 2.0 (AU), for the conditions implied).

Figure I is a graph of q_{\min} and c , as functions of m , for the information described above.

Figure II is a polar plot of $(q \text{ (AU)}, \theta^{\circ})$ for values of μ (or m) based on a fixed off-set distance (c) of 1 AU. Since the curves are symmetric about $\theta^{\circ} = 0$, then c may be the off-set on either side of the radial (0°); this is a typical result for any value of c (within the range of possible q distances allowed).

Figure III shows q, θ boundaries for several of the values of m used here. That is, each boundary corresponds to a chosen value of m ($\leq m_{\text{lim}}$). This describes a limit in q for the allowable range in c (AU), at a fixed μ . It should be remembered that $q = 2.0$ AU represents the arbitrary upper limit for this quantity. Note that when $m < 30 \times 10^{-15}$ gr then $q > 2.0$ AU; i. e., the particle is subjected to a large enough radiation (back-pressure) so that it does not have sufficient kinetic energy to move in as close as 2.0 AU from the sun, even for a direct radial approach. (The direct solar approach describes the q_{\min} noted earlier). It should be apparent that if $V_{\infty} > 20$ km/sec then the corresponding q -values should be smaller; the particles would be able to move closer to the sun against radiation pressure.

Figure IV graphically depicts the FORBIDDEN ZONE for this problem's conditions and constraints. Each curve, sketched on the figure, corresponds to a selected value of m ($< m_{\text{lim}}$). These arcs describe the geometric envelopes mentioned earlier; they separate regions, in the vicinity of the sun, into which the particles may move from those in which they cannot (the FORBIDDEN ZONE). Due to the obvious symmetry of this situation these arcs are mirrored in the solar (apex) radial line.

TABLE I. Calculated Data

Assume m(gr)	Compute β	Compute μ (AU, DA)	Closest Approach* q_{\min} (AU)	Representative Data (Based on $c = 1\text{AU}$)		c(AU) (For $q = 2\text{AU}$)
				q (AU)	θ°	
$89.9508 * 10^{-15}$	1.0	0		1.0	90°	2.0
$85 * 10^{-15}$	1.01905	$-5.63685 * 10^{-6}$	0.0845	1.043	87.58°	1.956
$80 * 10^{-15}$	1.03985	$-1.17924 * 10^{-5}$	0.1768	1.0923	84.95°	1.91
$75 * 10^{-15}$	1.06247	$-1.84834 * 10^{-5}$	0.2771	1.1481	82.11°	1.86
$70 * 10^{-15}$	1.087182	$-2.57973 * 10^{-5}$	0.3867	1.2119	79.05°	1.80
$65 * 10^{-15}$	1.114373	$-3.38430 * 10^{-5}$	0.5074	1.2854	75.76°	1.73
$60 * 10^{-15}$	1.144506	$-4.27593 * 10^{-5}$	0.641	1.3706	72.23°	1.648
$55 * 10^{-15}$	1.178187	$-5.2755 * 10^{-5}$	0.7909	1.4708	68.42°	1.55
$50 * 10^{-15}$	1.218219	$-6.39792 * 10^{-5}$	0.9592	1.5887	64.38°	1.448
$45 * 10^{-15}$	1.259692	$-7.68428 * 10^{-5}$	1.152	1.730	60.06°	1.304
$40 * 10^{-15}$	1.310132	$-9.17681 * 10^{-5}$	1.376	1.9017	55.48°	1.12
$35 * 10^{-15}$	1.36976	$-1.094132 * 10^{-4}$	1.640	2.1135	50.64°	0.85
$30 * 10^{-15}$	1.44199	$-1.30784 * 10^{-4}$	1.9607	2.3808	45.57°	0.294
$25 * 10^{-15}$	1.53234	$-1.57519 * 10^{-4}$	2.3615	2.7281	40.26°	< 0
$20 * 10^{-15}$	1.65066	$-1.92531 * 10^{-4}$	2.8865	3.2	34.72°	< 0

*Closest Approach would correspond to $c = 0(\text{AU})$.

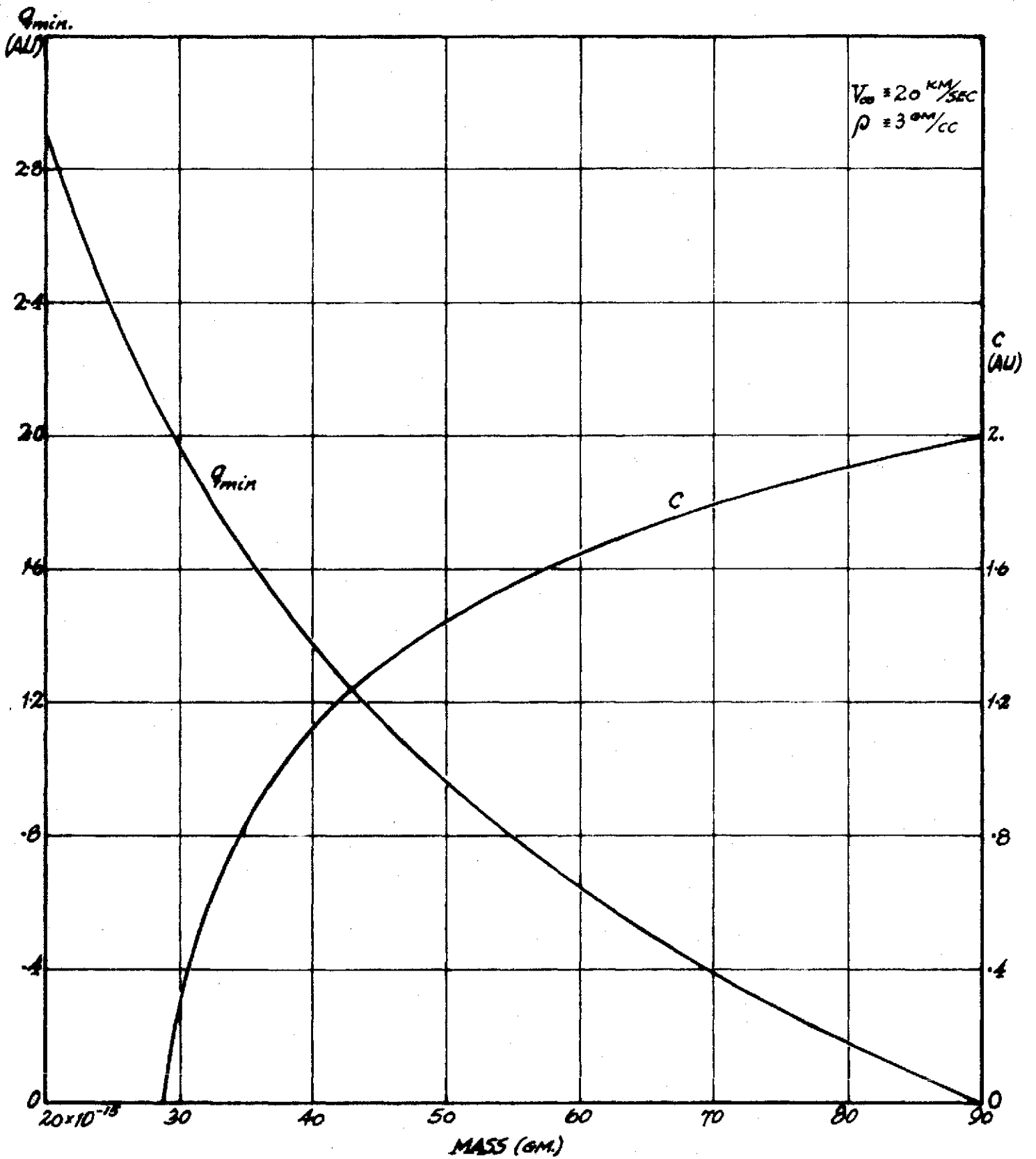


Figure I. Closest approach (q_{\min}) (on a radial) and offset distance (c), for $q = 2 \text{ AU}$, as a function of mass (gr).

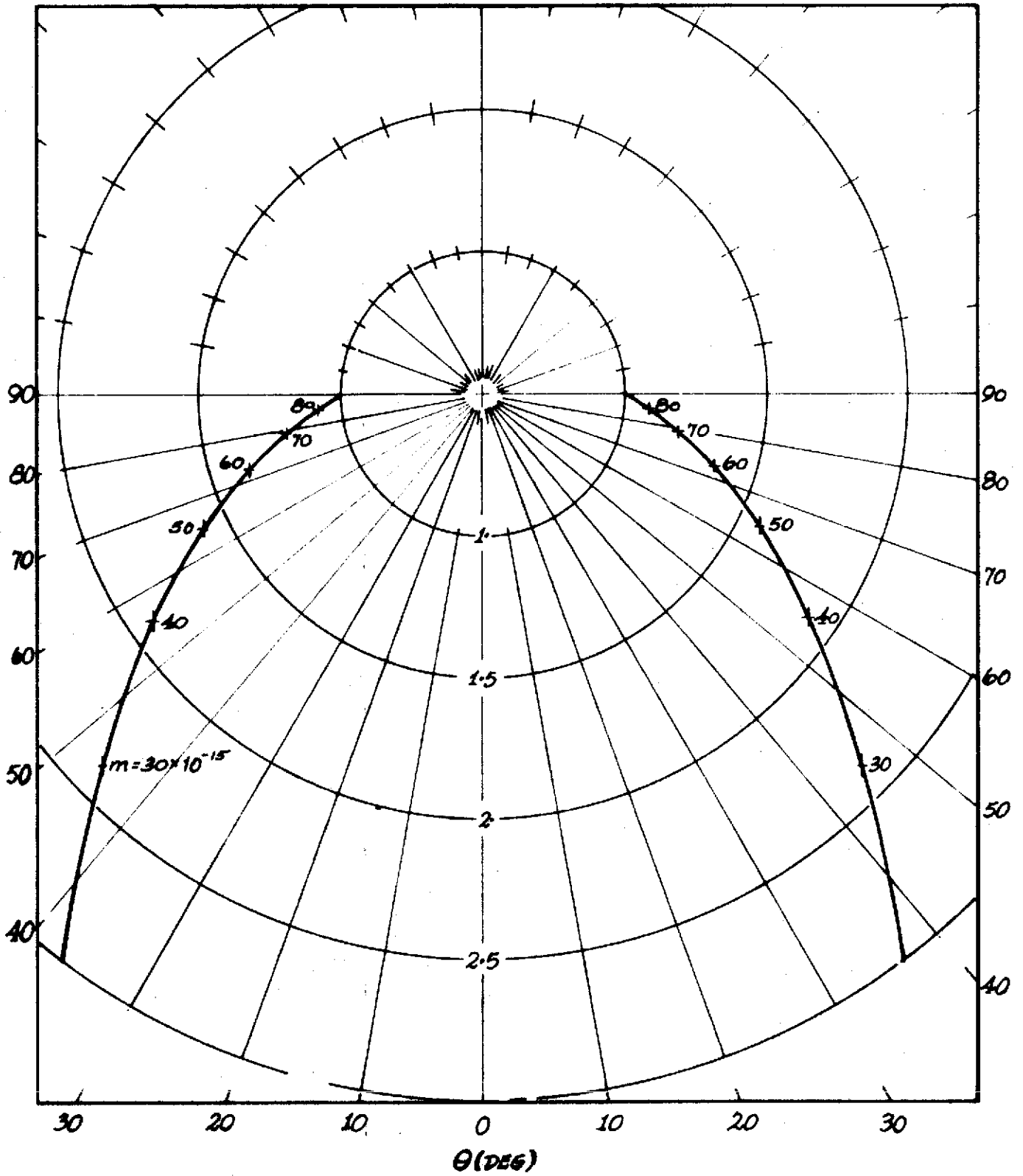


Figure II. Description of closest solar approach (η , θ) as a function of particle mass (m) - or equivalently (β or μ) - for a fixed offset distance (c) = 1.0 AU.

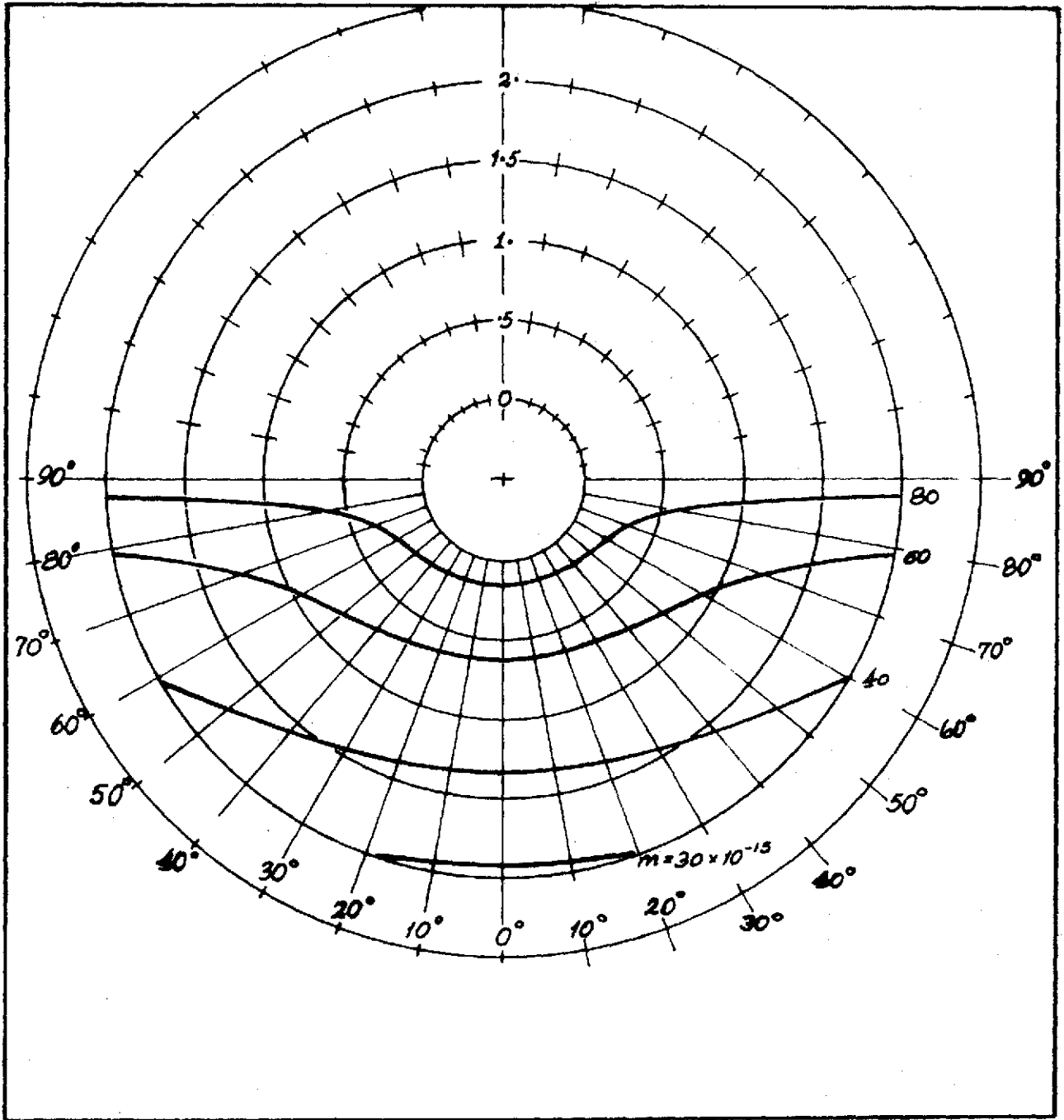


Figure III. A plot of q and θ for various values of c (c not shown). Note: each curve corresponds to a value of m , as specified.

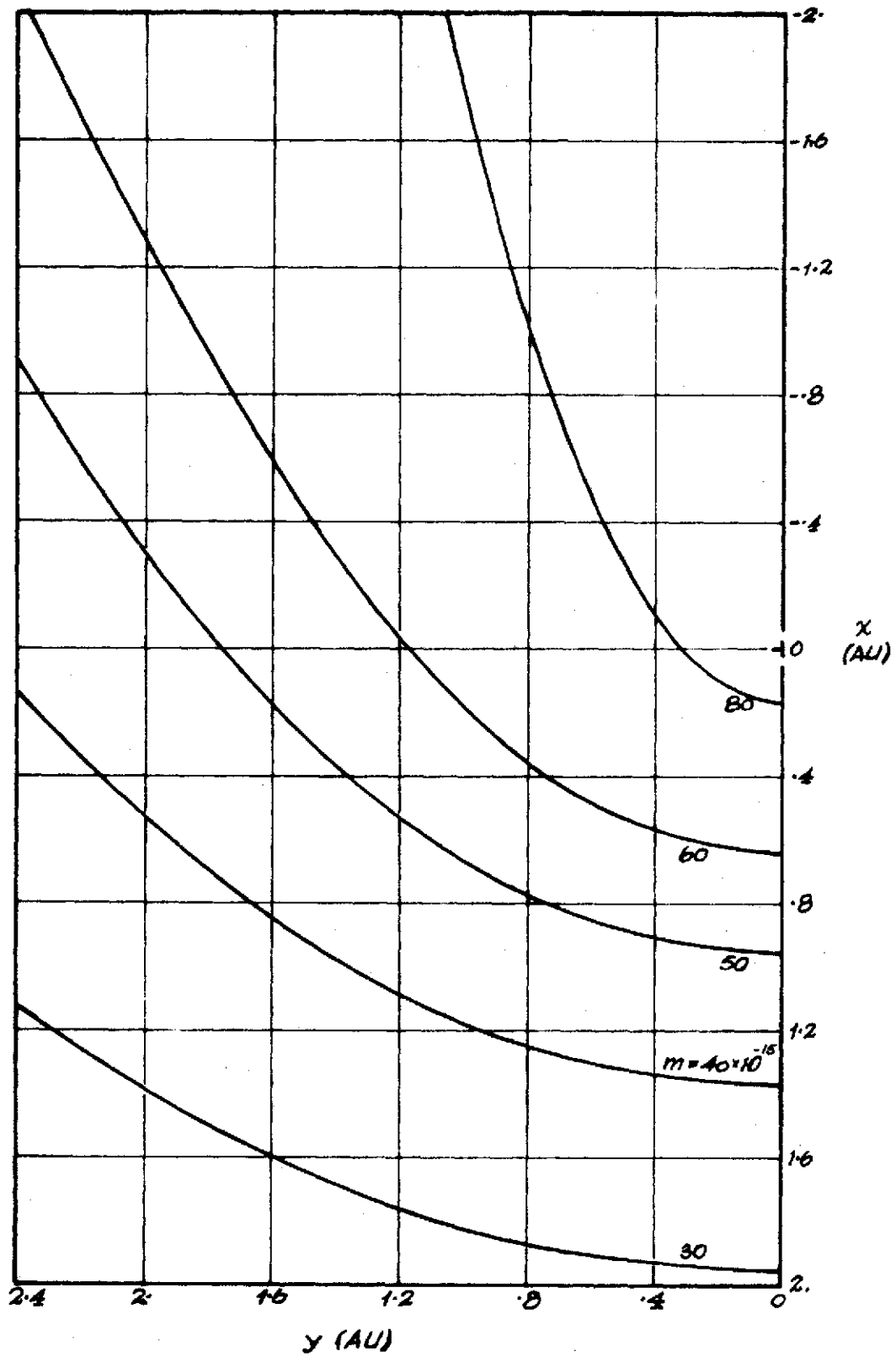


Figure IV. Graphic description of the "FORBIDDEN ZONE" for a specified case study.

Reference

- [1] Silverberg, Eric C., "Interplanetary Dust Streams: Observation by Satellites and Lidar", Thesis: University of Maryland, 1970.